THE WORK DONE ON THE SURROUNDING ATMOSPHERE BY SUBSIDING COLD AIR MASSES

By Norman A. Phillips

University of Chicago

(Manuscript received 8 October 1948)

ABSTRACT

The flux of energy due to the pressure force acting across the boundary of a subsiding mass of cold air is investigated. It is shown that for mean values of the subsiding motion of the order of -1 cm sec^{-1} or larger, energy is transferred from the cold air to the surrounding atmosphere. A method is developed whereby this flux across a portion of a frontal surface can be calculated from a three-dimensional frontal analysis, and this technique is then applied to a specific example. The importance of the addition of this energy to the current flowing around the cold air is discussed, and it is suggested that at least a portion of the energy for the indirect circulations which are often observed downstream is supplied by the direct circulation involving the subsiding cold air mass.

1. Introduction

It is generally accepted (see, for instance, [3]) that the conversion of the potential energy of the atmosphere into kinetic energy must play an important role in maintaining atmospheric motions against the dissipative effect of friction. The importance of this process was first investigated quantitatively by Margules [11]. He demonstrated, by considering a closed system in which the total energy remained constant, that certain gravitationally unstable arrangements of two air masses of differing densities could, through readjustment to a stable position, produce kinetic energy comparable to that observed in the storms of middle latitudes.

More recent investigations however (see, for example, [5; 7; 9; 12]) have emphasized the shortcomings of a closed system as a model when considering phenomena of the nature of developing cyclones and anticyclones. In this paper a process will be considered that is quite similar to that visualized by Margules in that a mass of cold air sinks, lowering its center of gravity and thereby decreasing its potential energy. It will be shown that this ordinarily implies a transfer of energy to the surrounding air, but since no solid walls are postulated as enclosing the two air masses, no quantitative statement can be made about any increase in the kinetic energy of the entire system, as could be done by Margules.

2. The sign of the work

If we have a mass of air Q which is separated from the surrounding air Q′ by the material surface A, the rate at which Q does work on Q′ is given by the surface integral [10]

$$\frac{dW}{dt} = \int\int_{A} p\boldsymbol{v}\cdot\boldsymbol{n}\,\delta a, \tag{1}$$

where p is the pressure, $\boldsymbol{v}$ is the (vector) velocity of the air at the surface, and $\boldsymbol{n}$ is the unit vector normal to A and directed from Q to Q′. Since A is a material surface (one through which no matter passes) the kinematic boundary condition requires that the component of $\boldsymbol{v}$ normal to the surface, *i.e.*, $\boldsymbol{v}\cdot\boldsymbol{n}$, be equal to C, the velocity of the surface in the direction normal to itself. A discontinuity in $\boldsymbol{v}$ across the surface is possible only in the components of $\boldsymbol{v}$ tangential to the surface, and therefore the velocity $\boldsymbol{v}$ in (1) may be either that of Q or Q′.

Let us now identify Q with a subsiding mass of cold air as shown in fig. 1. From this figure we see that

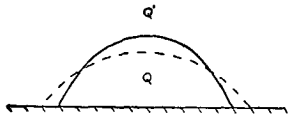

FIG. 1. Schematic cross section through a subsiding cold air mass. The solid line represents the profile at a time t while the dashed line represents the profile at a later time t'. The letters Q and Q' indicate respectively the cold and warm air masses.

$\boldsymbol{v}\cdot\boldsymbol{n}$ is positive in the lower levels (high pressure) and negative in the upper levels (low pressure). Since the integrand in (1) is this quantity multiplied by the pressure p, it would seem that the integrated effect of $p\boldsymbol{v}\cdot\boldsymbol{n}$ would be positive, with Q doing work on Q′. However, the subsidence of Q implies that Q will be compressed into a smaller volume. This must mean that more warm air replaces cold air by volume in the upper levels than cold air replaces warm air in the lower levels, and the possibility then exists that this

effect may be so pronounced as to overbalance the "weighting" of $\boldsymbol{v}\cdot\boldsymbol{n}$ by p. A consideration of the energy changes occurring within Q will demonstrate to us, however, that the subsidence of Q must be accompanied by an improbably large pressure rise throughout Q in order that (1) be negative.

We first express (1) as a volume integral by means of Gauss' theorem:

$$\frac{dW}{dt} = \int\int_{Q}\int \nabla\cdot p\boldsymbol{v}\,\delta\tau$$

$$= \int\int_{Q}\int (\boldsymbol{v}\cdot\nabla p + p\nabla\cdot\boldsymbol{v})\,\delta\tau. \quad (2)$$

$-\nabla p$ is the three-dimensional pressure gradient and $\nabla\cdot\boldsymbol{v}$ is the three-dimensional divergence of $\boldsymbol{v}$. If we introduce the equation of continuity, $d\rho/dt + \rho\nabla\cdot\boldsymbol{v} = 0$, and assume adiabatic motion,

$$\rho^{-1}\,d\rho/dt = (c_v/c_p)p^{-1}\,dp/dt,$$

(2) is readily transformed into the expression

$$\int\int_{Q}\int\left[(1 - c_v/c_p)\boldsymbol{v}\cdot\nabla p - (c_v/c_p)\frac{\partial p}{\partial t}\right]\delta\tau. \quad (3)$$

Splitting the term $\boldsymbol{v}\cdot\nabla p$ into two terms corresponding to the vertical and horizontal components of $\boldsymbol{v}$, and introducing $c_v/c_p = 0.71$ gives us

$$\frac{dW}{dt} = 0.29\int\int_{Q}\int\left(w\frac{\partial p}{\partial z} + \boldsymbol{v}_h\cdot\nabla_h p - 2.45\frac{\partial p}{\partial t}\right)\delta\tau, \quad (4)$$

where w and $\boldsymbol{v}_h$ are the vertical and horizontal components of $\boldsymbol{v}$, and $\nabla_h p$ is the horizontal component of ∇p.

In a subsiding air mass ($w < 0$) the first term in the integrand of (4) will be positive, while the other two may be positive or negative. Since we are attempting to demonstrate that (4) is positive, we shall assume a large negative mean value for the term $\boldsymbol{v}_h\cdot\nabla_h p$ and then see what mean value of the pressure tendency is needed in order to make the integrand of (4) equal to zero for a given value of w. It will appear that even with this large negative value for $\boldsymbol{v}_h\cdot\nabla_h p$, a large positive value of the pressure tendency is yet required to offset the positive effect of a small negative value of w. As mean values we assume

(*a*) $w = -1.5$ cm sec^{-1}. This corresponds roughly to a value of 0 cm sec^{-1} at $z = 0$ and -6 cm sec^{-1} at $z = 6$ km (thus agreeing qualitatively with the values found by Fleagle [6]).

(*b*) $\boldsymbol{v}_h\cdot\nabla_h p = -2\times10^{-5}$ cb sec^{-1}. This corresponds to a horizontal acceleration of about 40 m sec^{-1} (12 hr)$^{-1}$ and a geostrophic wind speed of about 20 m sec^{-1}.

(*c*) $\partial p/\partial z = -1\times10^{-2}$ cb m^{-1}.

Substituting these values in (4) we find that the critical value of $\partial p/\partial t$ for which (4) is zero is $+5.3\times10^{-5}$ cb sec^{-1} or about $+6$ mb (3 hr)$^{-1}$. In his study of vertical motion in selected cyclones over North America, Fleagle [6] found that the maximum pressure rise was situated to the rear of the trough and at a height of about 8 km. This maximum pressure rise was about 10 mb (12 hr)$^{-1}$ and decreased downward. One is then justified in concluding that the subsidence of cold air masses under the conditions discussed above ordinarily implies a transfer or flux of energy from the subsiding mass to its surroundings. In terms of the energy changes in the subsiding mass, we may infer that there is then such a large decrease in its potential energy that not only can it increase its internal and kinetic energy, but it must also do work on the surrounding air.

3. Measurement of the work from isobaric charts

In this section a method is derived for the evaluation of the integrated effect of (1) over the 12-hour period between upper-air observations. Since the velocity $\boldsymbol{v}$ is difficult to determine accurately, we avail ourselves of the kinematic boundary condition as discussed in the beginning of section 2 and write (1) in the form,

$$\frac{dW}{dt} = \int\int_{A} p\boldsymbol{C}\cdot\boldsymbol{n}\,\delta a, \quad (5)$$

where we no longer restrict the material surface A to be closed. The vector $\boldsymbol{C}$ may then be replaced by any other velocity $\boldsymbol{C}'$ which has everywhere on A the same normal component $\boldsymbol{C}'\cdot\boldsymbol{n}$ as does $\boldsymbol{C}$. In particular we may choose $\boldsymbol{C}'$ to be the velocity of a point which remains in the frontal surface, the pressure surface P, and the vertical plane normal to the front (see fig. 2).

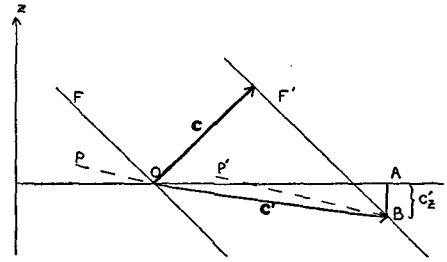

FIG. 2. Velocities at a frontal surface. The plane of the paper is vertical and normal to the front F. The normal rate of motion of the front is then represented by $\boldsymbol{C}$. P and P′ mark the intersection of the normal vertical plane with a given isobaric surface at times t and t'.

The horizontal component C_h' of $\boldsymbol{C}'$ is then the rate at which the front moves normal to itself on a *chart* of the isobaric surface P and is given by the line segment OA in fig. 2. The vertical component C_z' of $\boldsymbol{C}'$ is given by the line segment AB and is ordinarily much smaller than C_h', being of the order of 5×10^{-3} m sec^{-1} or less.

We now consider the frontal surface A as being parameterized by the variables p (pressure) and s, where s is the arc length measured along the line in space formed by the front and a pressure surface. We define s to increase as we progress along this line in an upright manner keeping the cold air to our left (see fig. 3). The surface integral we are investigating

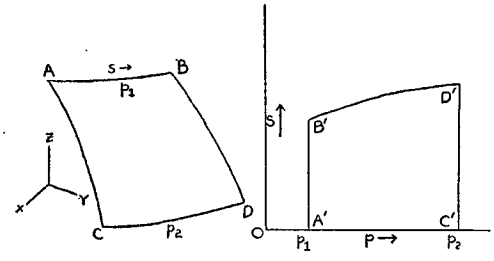

FIG. 3. Representation of a portion of a frontal surface by the parameters p and s. The drawing on the left represents the surface in three-dimensional space while the drawing on the right is the area in p, s space into which the frontal surface is mapped.

may now be expressed in terms of p and s, as shown by Courant [4].

$$\frac{dW}{dt} = \int\int_A p\mathbf{C}'\cdot\mathbf{n}\,\delta a$$
$$= \int\int_A p\left[C_x'\frac{\partial(y,z)}{\partial(p,s)} + C_y'\frac{\partial(z,x)}{\partial(p,s)} + C_z'\frac{\partial(x,y)}{\partial(p,s)}\right]\delta p\,\delta s, \quad (6)$$

where C_x', C_y', C_z' are the three components of the vector $\mathbf{C}'$ and the other factors are the Jacobians of the indicated cartesian variables with respect to p and s. The orders of magnitude in the mts system of the terms in these Jacobians are as follows:

$$\partial z/\partial p \approx 10^2, \quad \partial x/\partial s \approx 1, \quad \partial y/\partial s \approx 1$$
$$\partial z/\partial s \approx 10^{-4}, \quad \partial x/\partial p \approx 10^{-2}, \quad \partial y/\partial p \approx 10^{-2}.$$

It is apparent then that the last term in the integrand of (6) may be neglected[1] (especially so since C_z' is small), as may be the products in the first two Jacobians which do not contain the factor $\partial z/\partial p$. Introducing the hydrostatic equation (assuming that the front is a first or higher order of discontinuity with respect to density) and the equation of state, we then have

$$\frac{dW}{dt} \approx \frac{R}{mg}\int\int T\left(C_x'\frac{\partial y}{\partial s} - C_y'\frac{\partial x}{\partial s}\right)\delta p\,\delta s, \quad (7)$$

where g is the acceleration of gravity, T the temperature, and $R/m = 287$ kj ton^{-1} deg^{-1} is the gas constant for dry air. In (7), s is the arc-length along the line formed in space by the front and a pressure surface. If we now define l to be the arc length along the frontal line on an isobaric chart, (7) can be changed to

$$\frac{R}{mg}\int\int T\left(C_x'\frac{\partial y}{\partial l} - C_y'\frac{\partial x}{\partial l}\right)\delta p\,\delta l.$$

The term in parentheses is equal to C_h', the normal rate of motion of the frontal line on the isobaric chart. Since the frontal surface is quasi-isentropic, T may be considered as a function of p alone (using some average value of T along the front on each isobaric surface) and we finally obtain

$$\frac{dW}{dt} \approx \frac{R}{mg}\int T\int C_h'\,\delta l\,\delta p, \quad (8)$$

where we first integrate with l and then with p.

The integral of C_h' with respect to l is the rate at which area is being swept out on the isobaric chart by the frontal line. If we then integrate (8) with respect to time we get

$$W \approx \frac{R}{mg}\int T\int\int C_h'\,\delta l\,dt\,\delta p, \quad (9)$$

the work done through pressure forces by the cold air Q on the warm air Q′ across the frontal surface A during the time t. In (9) we have also averaged T with respect to time, so that T is now a function of p only. If we have a set of isobaric charts for the times t and t' on which the position of the front is marked, (9) may be easily computed. Fig. 4 shows how the

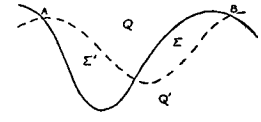

FIG. 4. Successive positions of a front on the same isobaric chart. The solid line is the position at time t and the dashed line is the position at a later time t'. Cold air (Q) has replaced warm air (Q′) in the area Σ while warm air has replaced cold air in the area Σ′.

frontal position on a given isobaric chart might appear at these two times. The area Σ minus the area Σ′ is then equal to the expression $\int\int C_h'\,\delta l\,dt$, where we consider only the frontal surface between the points A and B. If we then measure this for various isobaric charts by using a planimeter, multiply the area values so obtained by $RT(mg)^{-1}$, and then plot these products as a function of pressure, the area enclosed by the resulting curve will be (9).

4. Application to an actual case

Two principal difficulties were met in applying (10) to an actual case. First, the "front," defined as the upper surface of the stable layer representing the frontal *zone*, may be difficult to locate objectively, especially in the levels above 500 mb. This difficulty was obviated by adopting the convention that in

[1] Strictly speaking, this involves the more stringent assumption that

$$\int\int_A pC_z'\frac{\partial(x,y)}{\partial(p,s)}\,\delta p\,\delta s \ll \int\int_A p\left[C_x'\frac{\partial(y,z)}{\partial(p,s)} + C_y'\frac{\partial(z,x)}{\partial(p,s)}\right]\delta p\,\delta s.$$

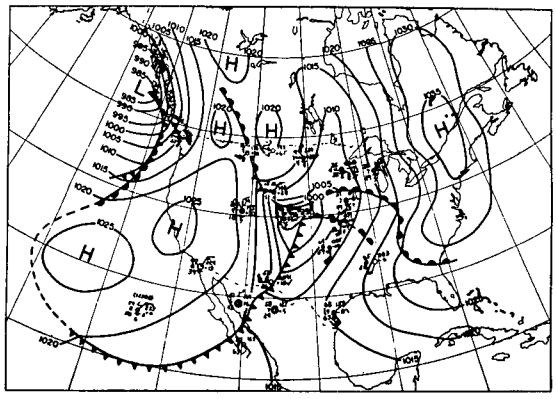

FIG. 5. Surface weather map for 0630 5 February 1946. Dashed lines are used where the frontal analysis is less accurate.

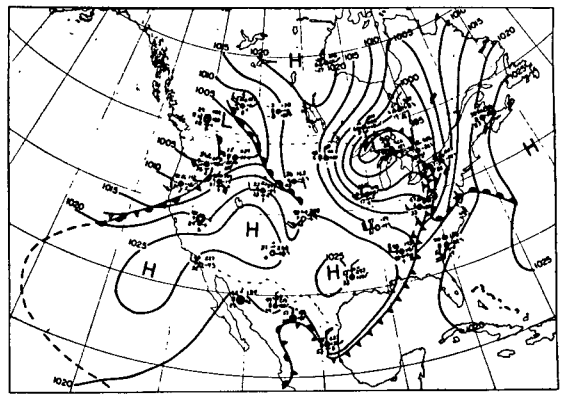

FIG. 6. Surface weather map for 1830 6 February 1946.

those regions where no stable layer was present on the radiosonde curves, the frontal surface coincided with an appropriate isentropic surface. (Stable layers which could be considered as representing the frontal zone were found on about 85 per cent of the soundings, with many of the remaining 15 per cent occurring in the upper portions of the cold front, where Bjerknes and Palmén [2] have noted the existence of strong baroclinity in the warm air adjacent to the front.)

The situation investigated was that existing over the central and western United States during the period of 5–6 February 1946. Surface synoptic charts for the beginning and end of the period are reproduced in figs. 5 and 6. On these figures two frontal systems are to be found: the *polar front* which marks the forward edge of the relatively deep polar air mass, and the *arctic front* to the north which denotes the boundary of the shallower layer of cold air formed over the northern continents in winter. The polar front is the front across which the work done by the pressure forces will be computed. It is evident from these maps that the front intersected the surface of the earth at a variety of pressures and therefore its accurate representation on a pressure chart for say 1000 mb would be quite complex. The following procedure was used to overcome this difficulty. The areas on the surface charts (including those for 1830[2] February 5 and 0630 February 6 which are not reproduced) corresponding to Σ and Σ' in fig. 4 were measured as if the surface charts had been isobaric charts. It was then assumed that the motion of the front given by the surface charts occurred at the pressure in the standard atmosphere corresponding to the average height above sea level of the frontal line on the surface charts. This average height was estimated by determination of the height at regular intervals along the frontal line. No motion was assumed to occur at pressures higher than this value.

Isobaric charts were analysed for the 850-, 700-, 600-, 500-, 400-, 300-, and 200-mb levels for the observation times of 0300 and 1500 on the 5th and 6th of February. The 500-mb charts for 0300 on the 5th and 1500 on the 6th are shown in figs. 7 and 8. These charts indicate clearly the increase in the geostrophic wind (and presumably the actual wind) above the cyclone during its development. On the first of these the separation between the polar and tropical air masses is very clear, while in the second chart the polar air has sunk below the 500-mb level except far to the north in Canada. The type of analysis used in these charts was patterned after that used by Bjerknes and Palmén [2] in their analyses of European cyclones,[3] and to aid in locating the front on the isobaric charts, 24 atmospheric cross sections were analysed, two of them being reproduced in fig. 9.

During the period of study a cyclone developed east of the Rockies in western Nebraska, deepened as it moved northeastward to the Great Lakes, and began to fill in the lower layers toward the end of the period.[4] The cold air (playing the role of Q) to the west and north of this storm was accompanied by a cold trough at the beginning of the period (fig. 7) and by a closed low-pressure system at the end of the period (fig. 8). The subsiding character of the motion of this air mass, as described above, is corroborated by a comparison of the minimum temperature of − 40C in the northwestern United States on fig. 7 with the corresponding temperature of − 30C southwest of Lake Michigan on fig. 8. Further evidence is presented in fig. 9, consisting of a cross section through the southern portion of the tongue of cold air. On cross section (A) for 0300 Feb. 5, there is a large lapse rate of temperature with height in the cold air, resulting in a remarkably intense frontal inversion of 10 degrees at station 278. This portion of the cold air has evidently been lifted just prior to this time, because the relative humidity

[2] All times in this paper refer to Greenwich Civil Time.

[3] Frontal analysis on isobaric charts also formed the subject of a series of lectures given by Professor Palmén at the University of Chicago during the fall of 1947.

[4] This storm produced severe dust storms and blizzards in the Mississippi Valley, and has been described previously [13].

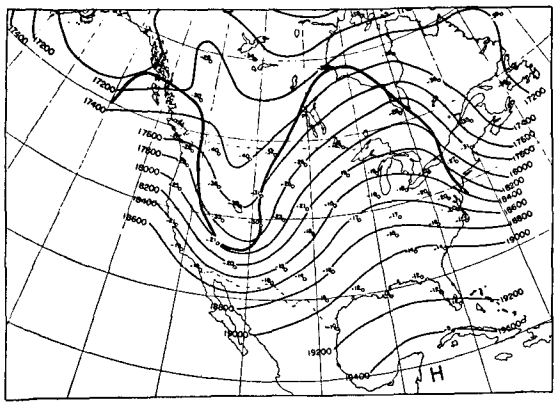

FIG. 7. 500-mb pressure contour chart for 0300 5 February 1946. Thin solid lines are height contours in intervals of 200 ft and heavy solid lines mark the upper surface of the frontal zone between polar and tropical air. Temperatures (C) are plotted by the station circles.

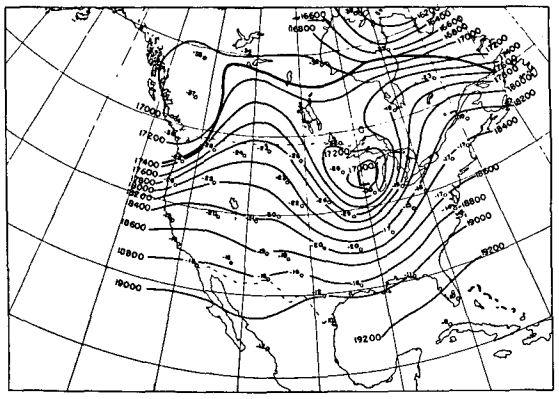

FIG. 8. 500-mb pressure contour chart for 1500 6 February 1946.

was high (not shown). The humidity decreased through the inversion, indicating that the principal reason for the intensity of the inversion was probably the combination of rising motion in the cold air and subsiding motion in the warm air above. During the next twelve hours a great change takes place, as is evident from cross section (B) for 1500 on February 5. The lapse rate within the cold air is now very stable, and the frontal inversion has weakened accordingly. This stabilization undoubtedly occurred because of the strong subsidence which took place in the polar air (witnessed also by the decrease in relative humidity, although this is not shown on fig. 9).

The pressure contours of the frontal surface at 0300 and 1500 on the 5th and 6th of February as transcribed from the corresponding isobaric charts are shown in figs. 10–13. In view of the descending motion of the cold air, the discussion in section 2 would now lead us to expect that the cold air mass has done work on the surrounding warm air during this process. The numerical results obtained by application of (9) to the frontal contour charts, as described at the end of section 3, are given in table 1. The last column in table 1 has then been plotted against pressure in fig. 14 for each 12-hr period. The area enclosed by each of these curves and the vertical zero line on fig. 14

TABLE 1. Computations for the calculation of the work done across the frontal surface.

Period	p (cb)	$\iint C_h' \delta l \, dt$ (10^{10} m^2)	T (K)	$\frac{RT}{mg}\iint C_h' \delta l \, dt$ (10^{14} m^3)
0300	40.0	−10.48	229.8	−7.05
Feb. 5	50.0	−10.56	244.8	−7.57
to	60.0	− 4.80	257.4	−3.62
1500	70.0	2.18	269.3	1.72
Feb. 5	85.0	13.38	283.3	11.10
	97.5 (sfc)	20.84	290.5	17.73
1500	50.0	−12.54	244.2	−8.97
Feb. 5	60.0	− 7.86	257.2	−5.92
to	70.0	0.87	268.6	0.69
0300	85.0	10.40	282.9	8.61
Feb. 6	99.5 (sfc)	18.73	291.5	15.99
0300	50.0	− 4.45	244.2	−3.18
Feb. 6	60.0	− 4.49	257.2	−3.38
to	70.0	0.56	268.6	0.44
1500	85.0	11.35	282.9	9.40
Feb. 6	99.7 (sfc)	18.69	291.5	15.96

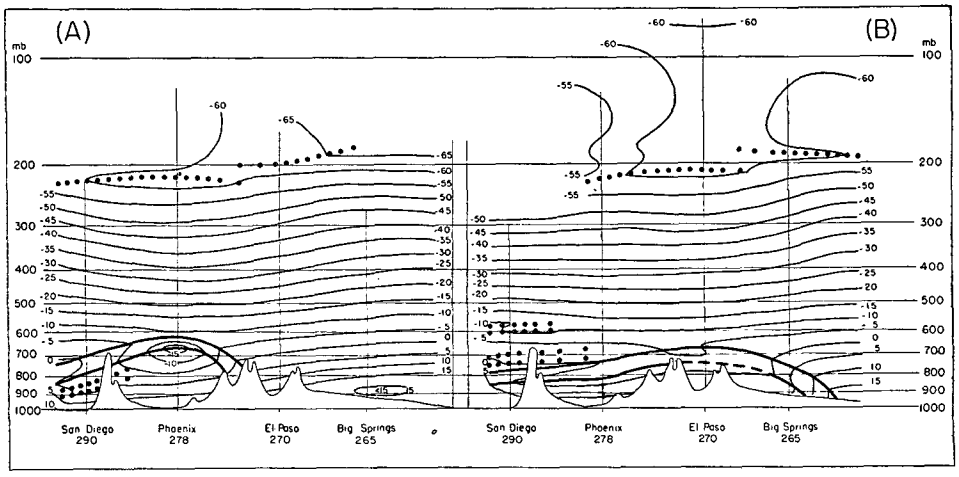

FIG. 9. West–east cross sections through the southern end of the subsiding cold dome at 0300 February 5 (cross section (A)) and at 1500 February 5 (cross section (B)). Heavy solid lines mark the boundary of the frontal zone, dotted lines mark subsidence inversions and tropopauses, and thin solid lines are isotherms.

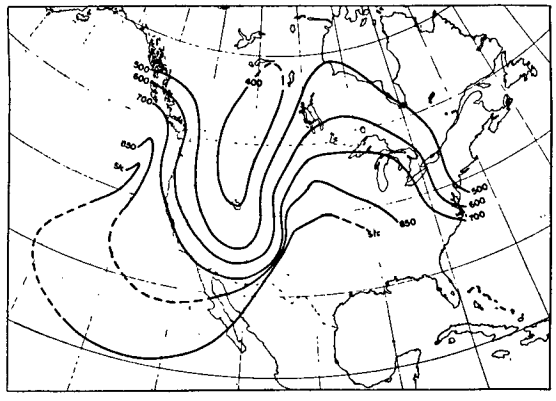

FIG. 10. Pressure contours of the frontal surface at 0300 5 February 1946. Contours are dashed where the frontal surface was indistinct or where data were especially scarce. The line marked *sfc* represents the intersection of the front with the ground.

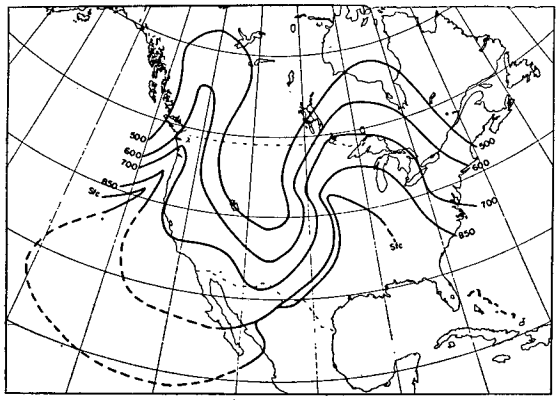

FIG. 11. Pressure contours of the frontal surface at 1500 5 February 1946.

then gives the amount of work done across this portion of the front by the cold air during the respective 12-hr period. (Areas to the left of the vertical zero line are negative, and areas to the right are positive.) These values are tabulated in table 2.

TABLE 2. Work done across the frontal surface during the three 12-hr periods.

Period	Work (10^{16} kj)
0300 Feb. 5–1500 Feb. 5	1.1
1500 Feb. 5–0300 Feb. 6	0.9
0300 Feb. 6–1500 Feb. 6	1.9*
Average	1.3

* This larger value reflects the increase in the mass of the cold air underneath the portion of the frontal surface to which the calculations were applied. This increase in mass can be inferred from fig. 6 and is apparent on fig. 14.

5. Interpretation

It is interesting to consider the order of magnitude of the quantities listed in table 2. Are they insignificant amounts of energy as far as the atmosphere is concerned, or are they of some importance?

To obtain some idea of the answer to this question, let us assume that the westerlies (to the south of the polar front) can be approximated by a mass of air which:

a. encircles the globe between 25° and 50°N,
b. is of a depth H equivalent to a pressure difference of 90 cb, and
c. has a "root mean square" wind speed of 20 m sec^{-1}.

The total kinetic energy of this mass of air is then given quite closely by

$$\tfrac{1}{2}\int_{25°}^{50°} a\,\delta\phi \int_{0}^{2\pi} a\cos\phi\,\delta\lambda \int_{a}^{a+H} \rho(20)^2\,\delta z,$$

where $a = 6.371 \times 10^6$ is the mean radius of the earth in meters. Substitution from the hydrostatic equation and carrying out of the indicated integration gives a value of 17.5×10^{16} kj.

Haurwitz [8] has estimated that the ratio of the kinetic energy in an atmospheric column to the amount of kinetic energy dissipated by friction within that column is such that the energy lost due to friction over a three-day period is equal to the kinetic energy of the column. His discussion involves the assumption that energy is being continually supplied from some other source so that the wind speed remains constant.

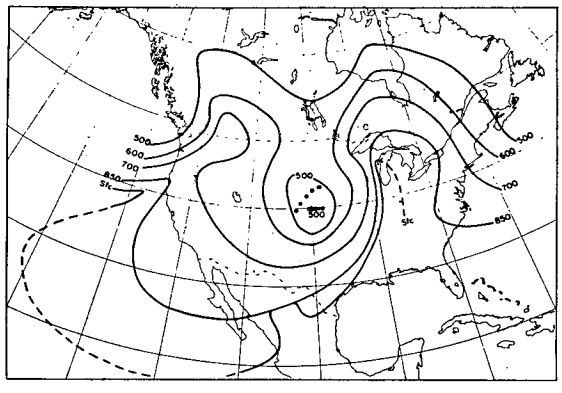

FIG. 12. Pressure contours of the frontal surface at 0300 5 February 1946.

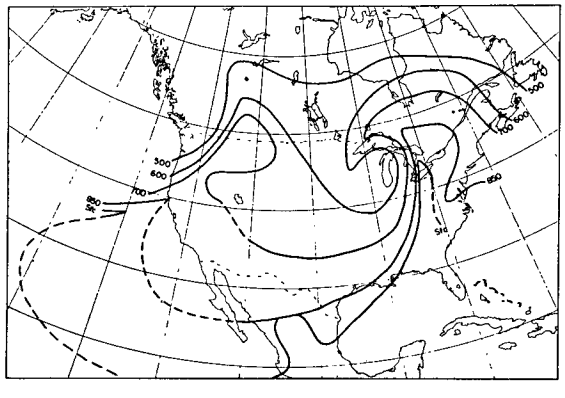

FIG. 13. Pressure contours of the frontal surface at 1500 6 February 1946.

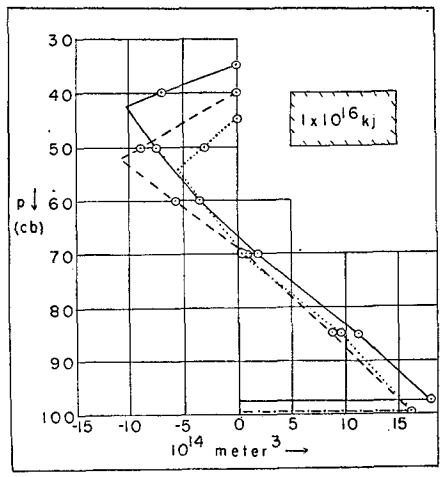

FIG. 14. Graph of the last column in table 1 plotted against pressure. The solid curve is for the period 0300–1500 5 February, the dashed curve is for the period 1500 5 February to 0300 6 February, and the dotted curve is for the period 0300–1500 6 February 1946. Area on this diagram is proportional to energy, the proportionality being given by the rectangle in the upper right corner.

If this reasoning is applied to our hypothetical belt of westerlies we find that 17.5×10^{16} kj must be supplied during a three-day period in order to maintain the kinetic energy. This amounts to about 3×10^{16} kj every 12 hr, or somewhat more than twice the average value shown in table 2.

It is important, however, to recognize that all of the energy added to the warm air cannot go into an immediate increase of its kinetic energy, and therefore it would seem that the subsidence of two such cold tongues is insufficient to replace the loss of kinetic energy in the warm air by friction. Obviously the center of gravity of the warm air mass is raised as it replaces the upper part of the cold air (fig. 1), and this will require an appreciable if not the major portion of the energy amounts listed in table 2. Additional energy is also required for the dynamic deformation of the tropopause observed to occur in these developments. Furthermore, the strong wind speeds in the upper troposphere in the vicinity of the subsiding cold air would presumably cause an increase of wind at a certain distance downstream to occur first in the upper troposphere. This would then, by the circulation theorem, be associated with an indirect transverse circulation acceleration in the neighborhood of this point acting to transfer part of the increased kinetic energy of the warm air back into potential energy of mass distribution.[5] It is apparent then, that the energy added to the warm air by the subsiding cold air appears in various forms and nothing can be said from the above analysis alone about the magnitude of any increase in the kinetic energy of the warm air.

Acknowledgment.—The writer wishes to acknowledge his indebtedness to Professor E. Palmén for his invaluable aid and the personal interest he has taken in the preparation of this study.

REFERENCES

1. Headquarters, Air Weather Service: Northern hemisphere historical weather maps, sea level and 500-mb. February, 1946.
2. Bjerknes, J., and E. Palmén, 1937: Investigations of selected European cyclones by means of serial ascents. *Geofys. Publ.*, **12**, no. 2, 62 pp.
3. Brunt, D., 1944: *Physical and dynamical meteorology, 2 ed.* Cambridge, University Press, 428 pp. (see p. 283).
4. Courant, R., 1936: *Differential and integral calculus*, vol. 2 (trans. E. J. McShane). New York, Interscience Publ., 682 pp.
5. Cressman, G. P., 1948: On the forecasting of long waves in the upper westerlies. *J. Meteor.*, **5**, 44–57.
6. Fleagle, R. G., 1947: The fields of temperature, pressure, and three-dimensional motion in selected weather situations. *J. Meteor.*, **4**, 165–185.
7. Goldie, A. H. R., 1937: Kinematical features of depressions. *Geophys. Mem.*, **8**, no. 72, 43 pp. (see p. 27 ff.).
8. Haurwitz, B., 1941: *Dynamic meteorology.* New York, McGraw-Hill Book Co., 365 pp.
9. Klein, W. H., and J. S. Winton, 1947: The path of the Atlantic hurricane of September 1947 in relation to the hemispheric circulation. *Bull. Amer. meteor. Soc.*, **28**, 447–452.
10. Lamb, H., 1932: *Hydrodynamics. 6 ed.* Cambridge Univ. Press, 738 pp.
11. Margules, M., 1905: Über die Energie der Stürme. *Jahrb. (Anh., 1903) Zentralanst. f. Meteor. Geodyn.*, Wien. (English translation in "The mechanics of the earth's atmosphere. A collection of translations by Cleveland Abbe," *Smithson. misc. Coll.*, **51**, no. 4, 533–595, 1910.)
12. Rossby, C.-G., 1945: On the propagation of frequencies and energy in certain types of oceanic and atmospheric waves. *J. Meteor.*, **2**, 187–204.
13. U. S. Weather Bureau, *Daily Weather Map*, March 29 and 30, 1946 (reverse side).

[5] Carson (J. E. Carson, "The variation of the horizontal solenoid concentration in the middle and low troposphere during cyclone formation," Master's thesis, University of Chicago, 1948), in studying the solenoid concentration in vertical planes immediately above the center of deepening cyclones, has found that the concentration of such solenoids (the "thermal wind") in the level 850–500 mb usually increases as the storm deepens. In the level 1000–700 mb, this phenomenon was not as well marked, the solenoid concentration decreasing as often as it increased. Some indication of an indirect transverse circulation downstream from the subsiding cold air mass of 5–6 February 1946 can be found on the 500-mb charts prepared by the Air Weather Service [1], although the data are insufficient to eliminate the effect of horizontal advection in increasing the south–north temperature gradient at that level.